Black Start and Fault Tolerant Operation of Isolated Matrix Converter for dc Microgrids

IECON 2022 – 48th Annual Conference of the IEEE Industrial Electronics Society | 978-1-6654-8025-3/22/$31.00 ©2022 IEEE | DOI: 10.1109/IECON49645.2022.9968735

Pietro Emiliani
Dep. of Electrical Power Engineering and Mechatronics
Tallinn University of Technology
Tallinn, Estonia
piemil@ttu.ee

Andrei Blinov
Dep. of Electrical Power Engineering and Mechatronics
Tallinn University of Technology
Tallinn, Estonia
andrei.blinov@taltech.ee

Andrii Chub
Dep. of Electrical Power Engineering and Mechatronics
Tallinn University of Technology
Tallinn, Estonia
andrii.chub@taltech.ee

Giovanni De Carne
Institute for Technical Physics
Karlsruhe Institute of Technology
Karlsruhe, Germany
giovanni.carne@kit.edu

Dmitri Vinnikov
Dep. of Electrical Power Engineering and Mechatronics
Tallinn University of Technology
Tallinn, Estonia
dmitri.vinnikov@taltech.ee

***Abstract*—This paper studies the transient behavior of a three-phase isolated bidirectional dc/ac converter operating as a rectifier. The purpose is to assess the viability of this converter for dc microgrid applications. A capacitor pre-charge method is developed to suppress inrush currents while charging the dc side capacitors during converter startup. The operation of the converter under grid fault transients is also studied, to assess the ability of the converter to maintain continuity of service to the dc microgrid in the case of grid undervoltage or loss of phase. A model of the converter was simulated on PSIM to validate the capacitor pre-charge method and grid fault responses.**

Keywords*—*dc microgrids, black start, PFC rectifier, three-phase

I. Introduction

Residential scale dc microgrids are a promising technology to facilitate the spread of dc-native distributed energy generators, such as photovoltaic panels or small wind turbines, allowing for greater renewable energy generation on a residential scale. Because of the variable nature of renewable energy resources, measures should be taken to ensure continuity of service to the residence. Energy storage devices such as electrical batteries can be installed to increase the on-site use of renewable energy. In this case, dc distribution reduces the number of energy conversion stages, therefore increasing efficiency. An active front-end (AFE) converter can interface the dc microgrid to the ac distribution grid, allowing for energy trading between the grids, depending on the generation and consumption of the residence [1], [2].

The three-phase high frequency link converter (HFLC) shown in Fig. 1, composed of a full bridge converter and one by three phase matrix converter (MC), is a candidate topology for realizing this connection. The HFLC directly converts energy from ac to dc, or vice versa, with a single stage of power conversion [3]-[7]. When operating as a rectifier, the MC feeds the transformer with a high frequency ac current which is rectified by the body diodes of the full bridge. Active switches are used on the dc side to allow for bidirectional power conversion, a necessary function for an isolated AFE, and enable synchronous rectification to reduce conduction losses. Unlike more conventional two stage solutions, there is no need for dc link capacitors to decouple power stages. However, capacitors are still necessary on the dc port of the AFE to provide a stable dc side voltage. Much of the existing literature focuses on improving steady state operation of the converter [8]-[10]. However, to be viable as an AFE in dc microgrids, it is essential that the converter can operate within its nominal limits under transient conditions like startup and grid side faults.

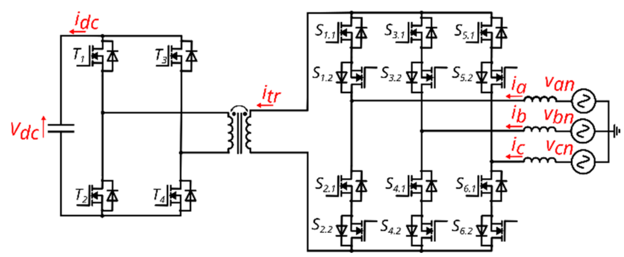

Fig. 1. Three-phase high frequency link converter.

Black start is the startup procedure of the converter when the dc port capacitors are fully discharged. This poses the well-known problem of inrush current, i.e., a transient overcurrent due to the discharged capacitors behaving like a short circuit that can damage converter components. Therefore, it is necessary to ensure that the current during startup is limited until the capacitors are fully charged and the converter can begin operating under normal conditions. In [11] a solid state circuit breaker is introduced capable of black starting the dc microgrid. In comparison, the HFLC is able to ensure black start using only control of the converter switches. The converter must also continue operating under grid side fault conditions, limiting the voltage drop on the dc side during the fault so that loads are not disconnected, and continuing operation even under some fault conditions like the disconnection of a phase.

The purpose of this paper is to give an overview on the capabilities of the HFLC applied to microgrids during transient conditions, specifically startup and fault. A simple black start control of the converter is employed to send controlled current pulses of current from the grid to the dc side capacitors, charging the dc side capacitors while limiting the current through the converter. The converter's operation during grid undervoltage conditions is studied. Finally, in the case of a phase disconnection the converter topology can be modified by controlling the switches to operate with only two legs, maintaining continuity of service during the fault.

II. Black Start

A. Current pulse generation

Matrix converters typically employ anti-series MOSFETS to achieve the required four quadrant operation. The ability to block voltage bidirectionally allows for full control of the current in the switches. Due to the presence of the inductors, interruption of current would cause large voltage spikes and potentially damage the converter. However, by opportunely controlling the timing of the switch commutations, it is possible to limit the current with natural commutations, making it possible to charge the dc capacitors with short pulses of current. Before the zero crossing of a line to line voltage, appropriate switches are turned ON to create a path for the current. This current is conducted through the body diodes of the dc side switches to charge the dc side capacitors. Only one of the two anti-series switches is turned ON, whereas the other conducts through the body diode, to allow only unidirectional current flow. Even in the case of fully discharged capacitors, the current is limited because of the polarity change of the grid voltage after the zero crossing. The switching sequence and general principles used to achieve black start of the dc microgrid are shown in Fig. 2 and Fig. 3 respectively.

The equivalent circuit, showing only one line to line voltage, V_{ab}, is shown in Fig. 2. By turning ON the switches $S_{1.2}$ and $S_{4.2}$ current begins to flow through the converter, and flows through the body diodes of switches T_1 and T_4 to charge the capacitors. As the switches are turned ON near the zero crossing of the grid voltage, the voltage applied to the inductor is small and the inductor limits the rise in current. After the zero crossing the voltage on the inductor changes polarity and the current begins to decrease, once it reaches zero the body diodes stop conducting and the active switch can be turned OFF with zero current switching (ZCS). For the zero crossing with opposite polarity, the active and passive switches on the ac side are swapped to allow unidirectional current flow in the opposite direction, and the body diodes of the opposite diagonal on the dc side (T_2, T_3) conduct.

The waveforms for line to line voltage, inductor current, and dc capacitor charge is shown in Fig. 3. The switches are turned ON at an angle α before the zero crossing. When the switches turn ON current begins to increase through the

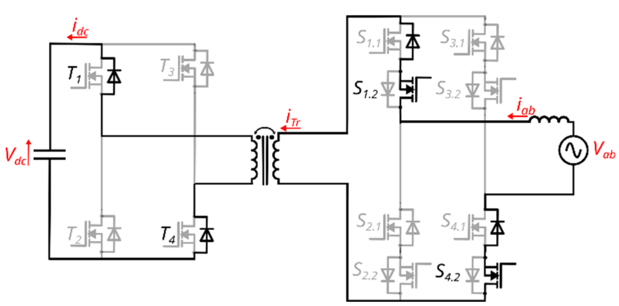

Fig. 2. Equivalent circuit when charging from line to line voltage Vab. Only $i_{ab}>0$ can flow as negative current would be blocked by the body diodes of $S_{1.1}$ and $S_{4.1}$.

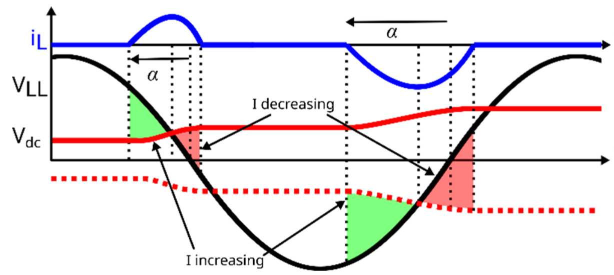

Fig. 3. Modulation angle. The switches turn on α degrees before the zero crossing of the voltage, enabling unidirectional current flow.

inductor and charge the capacitors. The equivalent circuit of the converter is simply a sinusoidal voltage source in series with an inductor and a capacitor. The voltage across the inductor V_L is the difference between the grid-side line to line voltage V_{ac} and the dc side capacitor voltage V_{dc}, with the switch turning ON at t = 0. For a positive to negative line to line voltage zero crossing, the inductor voltage V_L is calculated as

$$V_L = -V_{LL}\sin(\omega t+\alpha) - V_{dc}$$

With V_{LL} the amplitude of the line to line voltage. Given that the increase in capacitor voltage during each current pulse is small, the dc side capacitor voltage can be assumed constant during a current pulse, and the current can be expressed as

$$i_L = \frac{1}{L}\int_0^x V_L dt = \frac{V_{LL}}{\omega L}\left(\cos(\omega x+\alpha) - \cos(\alpha)\right) - \frac{V_{dc}x}{\mathrm{L}} \quad (1)$$

When there is current flow in the converter and the dc side body diodes are conducting, the dc side voltage is applied to the transformer magnetizing inductance. By alternating the sign of the current pulses for the two zero crossings in a period of line to line voltage, the current is alternatingly conducted through opposite diagonals of the dc side body diodes. As a result, the dc side voltage is applied to the magnetizing inductance with opposite polarity each conduction interval, avoiding saturation of the transformer. The current pulses should be controlled to respect both limits of maximum current, and maximum volt-seconds on the magnetizing inductance of the transformer. At the beginning of the black start, when the capacitors are fully discharged, then the maximum current limits the angle α . As the voltage of the dc side capacitors increases, the volt-seconds across the magnetizing inductance $V_{dc}x$ becomes more relevant. Once the absolute value of V_{LL} is less than the capacitor voltage the current begins to decrease until it reaches zero. The dashed red line shows the negative value of the capacitor voltage V_{dc}, for clarity when the current in the transformer is negative and polarity of the transformer is opposite.

TABLE I
Simulation Parameters

Simulation Parameter	Symbol	Value
Power	P	9.8 kW
Load resistance	R_{load}	50 Ω
dc voltage	V_{dc}	700 V
ac line to line voltage	V_{LL}	570 V
Grid filter inductance	L_g	1 mH
dc capacitance	C_{dc}	2 mF
Grid angular velocity	ω	$2\pi \cdot 50$

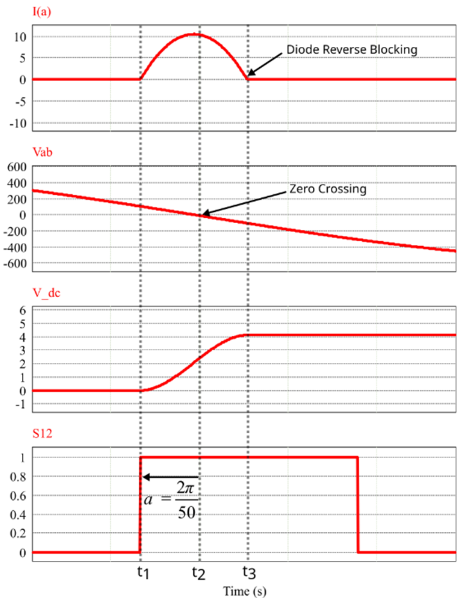

Fig. 4. Current pulse when the dc capacitors are fully discharged.

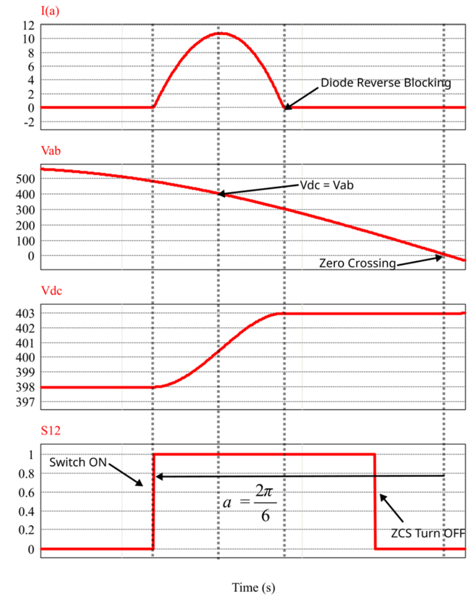

Fig. 5. Current pulse when the dc capacitors have charge (400 V).

As the capacitor voltage increases the angle alpha must be increased to apply a greater grid voltage. The black start was simulated on a PSIM model. The simulation parameters are given in Table I. Fig. 4 shows a current pulse when the capacitors are fully discharged. At angle $\alpha = 2\pi / 50$ before the zero crossing the switches $S_{1.2}$ and $S_{4.2}$ are turned on and begin to conduct current. The voltage across the capacitor begins to rise. The change in voltage polarity limits the current. During conduction the voltage of the discharged capacitor is applied to the transformer, so there is no risk of saturation. Once the current reaches zero the diodes undergo reverse recovery and begin blocking current. It is now possible to turn off the active switches with ZCS. As the switches are operating at grid frequency, the switching losses do not pose a significant issue. However, isolated matrix type topologies that operate with hard switching on the MC side suffer from transient overvoltages as there is no freewheeling path available in a bidirectional switch [12]. Therefore, ZCS protects the switches from transient overvoltages [13].

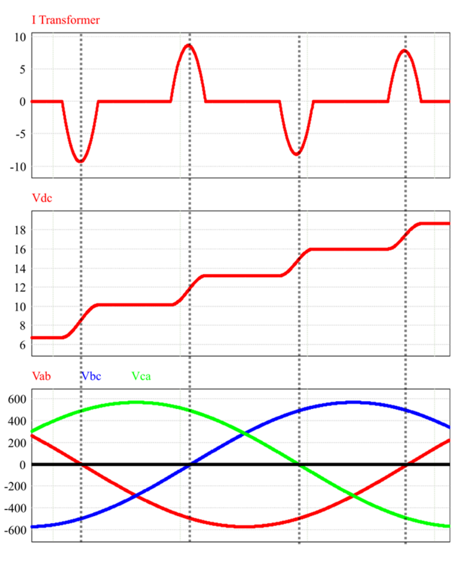

Fig. 6. Charging of dc side capacitors with current pulses. There are two current pulses per phase per grid period, for a total of six current pulses per grid period. Dashed lines show the zero crossing of the grid voltages.

Fig. 5 shows a current pulse when the capacitor is at 400V. In this case $\alpha = 2\pi / 6$. The maximum current is when Vac = Vdc. In this case there is no need for the zero crossing of the line to line voltage, as the capacitor voltage is enough to limit the current in the converter. As there is now significant voltage applied to the transformer during conduction, the current pulse duration should be limited to avoid saturation.

Fig. 6 shows the charging of the dc link capacitor during one grid period. As the capacitors are almost fully discharged the conduction intervals occur near the zero crossing to limit the current. By setting α according to (1) during the charging process, the nominal ratings of the converter, overcurrent and transformer saturation are avoided.

III. Fault Tolerance

Another concern for dc microgrid applications is the robustness of the converter, i.e., how well can it respond to faults on the grid and maintain a stable dc side voltage during a fault. The behavior of the converter was studied during a sudden undervoltage on the grid and the loss of a phase.

A. Converter Modulation

The HFLC is current fed, allowing for explicit control of the grid side currents. As the converter boosts voltage when rectifying, grid undervoltage does not present significant problems, as long as the control is able to respond in an appropriate time by increasing the ac side currents. A phase-shift modulation utilizes a quasiresonant (QR) state for favorable switching conditions is used. The sequence is described thoroughly in [14]. Fig. 7 shows a simplified representation of relevant waveforms during a switching period. As the topology has three ac legs with no neutral wire, all three grid side currents can be controlled by controlling

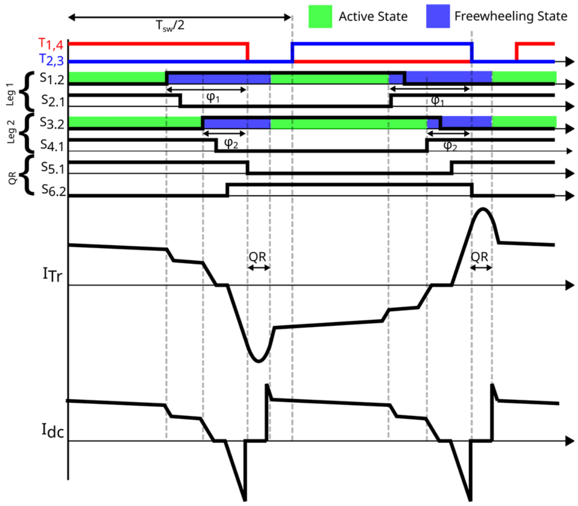

Fig. 7. Converter modulation principle. φ_1 and φ_2 are the angles between the turn on of the active switch in the respective leg and the turn off of the dc-side switches, initiating the QR phase.

the currents in two of the legs, by changing the angles φ_1 and φ_2. By decreasing the phase shift, the leg spends more time in the freewheeling state and the current through the inductor increases.

The converter is controlled with two nested PI loops, shown in Fig. 8. The outer loop controls the dc side voltage Vdc and sets current amplitude reference I, the inner controls the ac side currents by setting the phase shift angles φ_1 and φ_2 from which the gate signals are generated. $\overline{V_{ac}}$ and $\overline{I_{ac}}$ are the vectors of grid voltages and currents respectively.

B. Grid Undervoltage

A simulation was carried out where the grid voltage immediately fell to half of its value. After the step fall in grid voltages, the grid side currents must increase to maintain the voltage on the dc side. The regulator increases the current amplitude reference, and therefore increases the phase shifts, effectively lowering the duty cycle of the legs. The grid side currents do not immediately increase to the new reference as their rise is limited by the grid filter inductance, the combination of low current and low duty cycle immediately after the grid undervoltage fault cause the dc side capacitor voltage to rapidly drop until the grid side currents have time to increase. In the simulation there was approximately a 10 V drop in dc side voltage with 2 mF of capacitance. When the grid voltages returned to nominal value there was a 10 V overshoot. This is an acceptable transient in voltage given the expected tolerances of a dc microgrid.

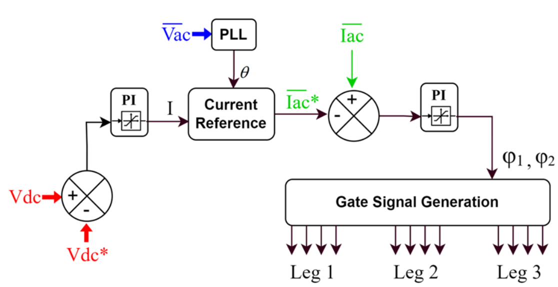

Fig. 8. Two nested PI regulators control ensure the dc side voltages tracks the reference by modifying the phase shift.

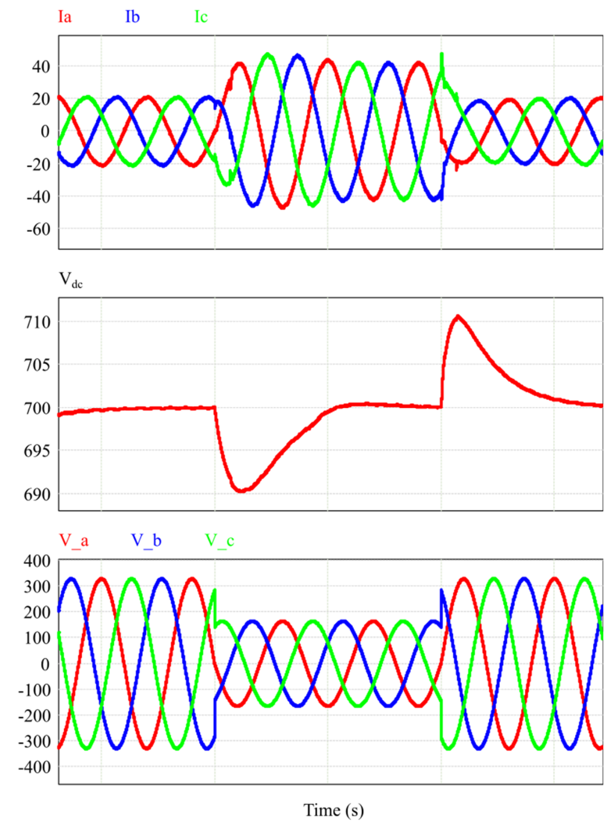

Fig. 9. Currents on ac side (Ia, Ib, Ic) and voltage on dc side (Vdc) during a step grid undervoltage.

value there was a 10 V overshoot. This is an acceptable transient in voltage given the expected tolerances of a dc microgrid.

C. Phase Disconnection

In the case of the sudden disconnection of a phase, it is possible to reconfigure the ac side of the converter, operating as if it were a two by two phase matrix converter by using two legs of the MC while keeping the switches of the disconnected phase open. After reconfiguration the converter essentially becomes the topology described in [13]. The reconfigured topology is shown in Fig. 10. The nominal power of the converter is reduced to two-thirds as only two legs are carrying current. Fig. 10 shows the simulation result of the disconnection of phase C and reconfiguration of the topology. There is a 100 Hz ripple on the dc capacitor voltage, as there is only one line to line voltage that can be used, and power cannot be transferred at the zero crossing of the voltage. However, this ripple is relatively small, +/- 5 V.

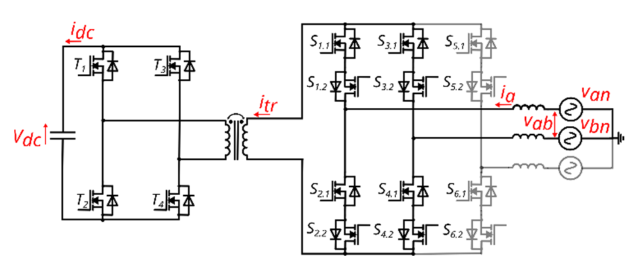

Fig. 10. HFLC topology reconfigured to operate with a single line to line voltage

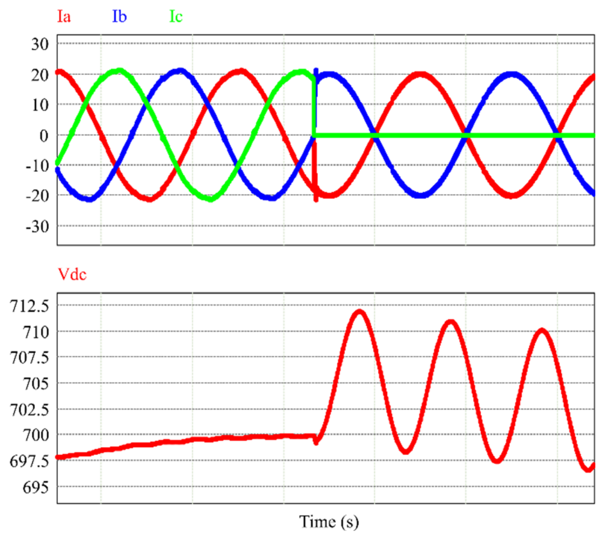

Fig. 11. Simulation result after a phase is disconnected and the converter reconfigures to operate with only two MC legs

As the two legs are operating within their nominal limits, the converter can operate in this mode indefinitely.

IV. Conclusion

This paper gives a preliminary overview of the capabilities of a three-phase HFLC during black start and fault transients in the context of operation in a dc microgrid. It was shown that the bidirectional switches allow for precharging of the dc side capacitors while respecting the overcurrent and transformer saturation limits, without any additional circuitry required. Two common fault conditions, grid undervoltage and phase disconnection, were simulated. As the converter boosts the voltage when operating as a rectifier, grid side undervoltage does not pose a significant problem. Even with relatively small dc side capacitance the voltage drop is acceptable for a dc microgrid. In the event of phase disconnection, the converter can be reconfigured to operate off of a single line to line voltage, maintaining two thirds of its nominal power indefinitely without overloading. The black start ability and fault tolerant operation of the converter make it a suitable candidate for dc microgrids.

Acknowledgment

This project has received funding from the European Union's Horizon 2020 research and innovation programme under the Marie Sklodowska-Curie grant agreement no. 955614.

References

[1] G. Pepermans, J. Driesen, D. Haeseldonckx, R. Belmans and W. D'haeseleer, "Distributed generation: definition, benefits and issues," *Energy Policy,* vol. 33, no. 6, pp. 787-798, 2003. J. Clerk Maxwell, A Treatise on Electricity and Magnetism, 3rd ed., vol. 2. Oxford: Clarendon, 1892, pp.68–73.

[2] Lasseter, R.; Akhil, A.; Marnay, C.; Stephens, J.; Dagle, J.; Guttromson, R., et al. (2002). Integration of distributed energy resources. The CERTS Microgrid Concept. *Lawrence Berkeley National Laboratory*

[3] T. Kawabata, K. Honjo, N. Sashida, K. Sanada and M. Koyama, "High frequency link DC/AC converter with PWM cycloconverter," *Conference Record of the 1990 IEEE Industry Applications Society Annual Meeting*, 1990, pp. 1119-1124 vol.2, doi: 10.1109/IAS.1990.152325.

[4] Korkh, O.; Blinov, A.; Vinnikov, D.; Chub, A. Review of Isolated Matrix Inverters: Topologies, Modulation Methods and Applications. Energies 2020, 13, 2394. https://doi.org/10.3390/en13092394

[5] A. Blinov et al., "High Gain DC–AC High-Frequency Link Inverter With Improved Quasi-Resonant Modulation," in IEEE Transactions on Industrial Electronics, vol. 69, no. 2, pp. 1465-1476, Feb. 2022, doi: 10.1109/TIE.2021.3060657.

[6] K. Tomida, K. Natori, J. Xu, N. Shimosato and Y. Sato, "A New Control Method to Realize Wide Output Voltage Range for Three Phase AC/DC Converter Based on Matrix Converter," 2022 International Power Electronics Conference (IPEC-Himeji 2022-ECCE Asia), 2022, pp. 96-101, doi: 10.23919/IPEC-Himeji2022-ECCE53331.2022.9806844.

[7] J. Afsharian, D. Xu, B. Wu, B. Gong and Z. Yang, "The Optimal PWM Modulation and Commutation Scheme for a Three-Phase Isolated Buck Matrix-Type Rectifier," in IEEE Transactions on Power Electronics, vol. 33, no. 1, pp. 110-124, Jan. 2018, doi: 10.1109/TPEL.2017.2661242.

[8] S. Norrga, S. Meier and S. Ostlund, "A Three-Phase Soft-Switched Isolated AC/DC Converter Without Auxiliary Circuit," in *IEEE Transactions on Industry Applications*, vol. 44, no. 3, pp. 836-844, May-june 2008, doi: 10.1109/TIA.2008.921430.

[9] A. Pal and K. Basu, "A Single-Stage Soft-Switched Isolated Three-Phase DC–AC Converter With Three-Phase Unfolder," in IEEE Transactions on Power Electronics, vol. 35, no. 4, pp. 3601-3615, April 2020, doi: 10.1109/TPEL.2019.2935875.

[10] F. Wu and X. Li, "Improved Modulation for Dual Active Bridge Based Three-Phase Single-Stage AC-DC Converter," 2019 IEEE Energy Conversion Congress and Exposition (ECCE), 2019, pp. 2135-2140, doi: 10.1109/ECCE.2019.8912679.

[11] Y. Zhou, Y. Feng, T. Liu and Z. J. Shen, "A Digital-Controlled SiC-Based Solid State Circuit Breaker with Soft-Start Function for DC Microgrids," 2018 9th IEEE International Symposium on Power Electronics for Distributed Generation Systems (PEDG), 2018, pp. 1-7, doi: 10.1109/PEDG.2018.8447563.

[12] A. Blinov, I. Verbytskyi, D. Peftitsis and D. Vinnikov, "Regenerative Passive Snubber Circuit for High-Frequency Link Converters," in IEEE Journal of Emerging and Selected Topics in Industrial Electronics, vol. 3, no. 2, pp. 252-257, April 2022, doi: 10.1109/JESTIE.2021.3066897.

[13] A. Blinov, D. Vinnikov, E. Romero-Cadaval, J. Martins and D. Peftitsis, "Isolated High-Frequency Link PFC Rectifier with High Step-Down Factor and Reduced Energy Circulation," in *IEEE Journal of Emerging and Selected Topics in Industrial Electronics*, doi: 10.1109/JESTIE.2021.3126226.

[14] P. Emiliani, A. Blinov, A. Chub, G. De Carne and D. Vinnikov "DC Grid Interface Converter Based on Three-Phase Isolated Matrix Topology with Phase-Shift Modulation" 2022 *IEEE* 13th International Symposium on Power Electronics for Distributed Generation Systems in press.